RSC Advances

Preparation of PVA Nanocomposites Using Salep-Reduced Graphene Oxide with Enhanced Mechanical and Biological Properties

Journal:	*RSC Advances*
Manuscript ID	RA-ART-06-2015-012190.R2
Article Type:	Paper
Date Submitted by the Author:	03-Oct-2015
Complete List of Authors:	Pourjavadi, Ali; Sharif university of technology, chemistry Pourbadiei, Behzad; Sharif University of Technology, Chemistry Doroudian, Mohadeseh; Sharif university of technology, Chemistry Azari, Shahram; National Cell Bank of Iran, Pasteur Institute of Iran
Subject area & keyword:	Polymers < Materials

RSC Advances

Paper

Preparation of PVA Nanocomposites Using Salep-Reduced Graphene Oxide with Enhanced Mechanical and Biological Properties

Ali Pourjavadi [a], Behzad Pourbadiei[a], Mohadeseh Doroudian [a], Shahram Azari[b]

Salep known as a biodegradable polysaccharide is hydrolyzed and used as either reducing agent and stabilizer for graphene oxide (GO). The functionalized reduced graphene oxide (f-rGO) is homogenously dispersed in an aqueous solution of poly (vinyl alcohol) (PVA). PVA based hydrogel and film nanocomposites are prepared and proposed as new biomaterials for tissue engineering applications. Mechanical properties of the film nanocomposites are investigated at various contents of f-rGO, glycerol and citric acid as a reinforcing agent, a plasticizer agent and a cross linking agent respectively. For the first time, chemically cross linked PVA hydrogels are synthesized using *N,N'*-methylenebisacrylamide (MBA) and ammonium persulfate (APS) without using hazardous monomers. Water absorbency and mechanical properties of the prepared samples have been enhanced considerably in comparison with the previous reports on PVA hydrogels. Chemical and physical characterization of the nanocomposites are carried out using Fourier transferred infrared spectroscopy (FTIR), X-ray photoelectron spectroscopy (XPS), X-ray powder diffraction (XRD), thermogravimetric analysis (TGA), scanning electron microscopy (SEM and field emission-SEM), tensile and compression mechanical tests. Cell culture on both of the film and hydrogel samples indicates that the synthesized nanocomposites have good biocompatibility and can be used as promising biomaterials with desired mechanical properties.

1. Introduction

Bionanocomposites have attracted great research interest in biomedical applications such as tissue engineering and drug delivery systems. Fabrication of novel biomaterials with remarkable mechanical properties, good biocompatibility and cell attachment is still challenged in tissue engineering studies. PVA based materials have been extensively used in biomedical applications including contact lenses [1], drug delivery systems[2] and substitutes for repairing the diseased or damaged articular cartilages[3], meniscuses and tendons[4] due to their biocompatibility, high hydrophilicity and good processability. Graphene with excellent electrical and thermal conductivity, high tensile modulus (1.0 TPa), ultimate strength (130 GPa)[5] and good biocompatibility has attracted great research interest in biological studies. Recently, fabrication of the polymer/graphene nanocomposites in order to improve the mechanical, electrical and thermal properties of the materials has been widely investigated. In order to regain the electrical properties of graphene, reduction of its precursor (GO) has been studied using various reducing agents[6, 7]. Reduced graphene oxide (rGO) sheets tend to form irreversible aggregation corresponding to the strong interplanar

[a] *Polymer Research Laboratory, Department Of Chemistry, Sharif University of Technology, Azadi Avenue,P.O.Box11365-9516, Tehran, Iran*

[b] *National Cell Bank of Iran, Pasteur Institute of Iran, Tehran, Iran*

interactions. Therefore, complicated surface modification is often needed to avoid the aggregation of rGO sheets during reduction process. Besides, natural hydrogels containing rGO show great potential as the 3D-matrices for cell culture, contact lenses, wound covering, vascular cell culture, vascular implanting, heart valves and cartilage substitutes[8, 9].

Many efforts have been done to improve the dispersion and interface interactions of graphene in the polymer matrix with both covalent and non-covalent modifications[10-12]. Various polysaccharides such as chitosan, cellulose and carrageenan have been used frequently in biomaterial scaffolds [13, 14] because of their hydrophilicity, biocompatibility and biodegradability. Moreover, due to the chemical similarity with heparin, polysaccharides show good hemocompatibility and suitable interaction with living cells. Several hydroxyl groups enable polysaccharides to interact greatly with proteins through covalent, electrostatic and hydrogen bonding[15] furthermore play an important role in maintaining the structure of the extracellular matrix. However, some major drawbacks such as low mechanical strength and improper processability restrict polysaccharides application in tissue engineering scaffolds. Accordingly, formation of the organic biopolymer/graphene nanocomposites is a promising strategy to enhance both biological and mechanical properties. For example, Qu et al. used a wet spinning method in order to fabricate regenerated cellulose fibres filled with low graphene loading[16]. Hu et al. functionalized reduced graphene oxide (rGO) by chitosan (CS), and then incorporated the CS-functionalized rGO into poly (vinyl alcohol) (PVA) to obtain the PVA-based nanocomposite films by a solution casting method[17].

Salep, a polysaccharide obtained from dried roots of orchids such as Orchis morio [18], is known to consist of D-glycopyranosyl and D-mannopyranosyl residues at a ratio of 1:3. Salep as a nontoxic and stable water-soluble polysaccharide extensively has been used at various fields by our research group[15, 19].

Taking these considerations into account, we aimed to synthesize reduced soluble GO by using salep instead of toxic reducing agents and then, to fabricate reinforced PVA nanocomposites. Eco-friendly hydrolyzed salep was used as both the reducing agent and the stabilizer to prepare functionalized reduced graphene oxide (f-rGO). Good dispersion of f-rGO in the aqueous phase of PVA through intermolecular interactions are mediated by the hydroxyl groups of salep on the surface of graphene. Both of the components are hydrophilic that lead to the multiple hydrogen bonding and the improving interfacial interactions between the f-rGO and PVA.

In this study, film nanocomposites were prepared by solution casting of an aqueous suspension of f-rGO and PVA. The mechanical performance of the films were studied in the presence of additives such as glycerol and citric acid. Biocompatibility and promotion in cell attachment associated with salep, processability of PVA and significant physical properties of f-rGO are the advantages of these film nanocomposites.

Currently, to the best of our knowledge, there have not been any reports on the chemical cross-linked hydrogels of PVA without addition of toxic monomers such as acrylic acid, methyl acrylate and acryl amid. Herein, hydrogel formation from PVA solution loaded with f-rGO was carried out using low

amount of MBA as a cross-linker. Interfacial bonding between hydroxyl groups of f-rGO and PVA facilitates water absorbency and mechanical strength of the hydrogels. Finally, the cytotoxicity tests revealed that we have been successful to synthesize environmentally friend nanocomposites for the production of biomaterials which are highly desirable for tissue engineering applications as well.

2. Experimental

2.1. Materials

Salep was purchased from a company in Iran (Mn = 1.17×10^6 g/mol, Mw = 1.64×10^6 g/mol (high Mw), PDI = 1.39, eluent = water, flow rate = 1 mL/min, acquisition interval = 0.43 s from GPC results). H_3PO_4 (85%), H_2O_2 (30%), dimethyl formamide (DMF), butanol, acetic acid (98%), *N,N'*-bisacrylamide (MBA), ammonium persulfate (APS), citric acid (ca), glycerol (gly), PVA (molecular weight: 145000 g/mol), all were purchased from Merck. Other solvents (NH_4OH, HCl, H_2SO_4 and acetone) were analytical grade. Deionized (DI) water was used for all experimental methods. Graphite purification was performed in an alkaline solution. In summary, 10 g of graphite was stirred in 20 mL of NaOH solution (25%) for 40 min and then heated at 300 ˚C for one hour. The resulting solid was washed with HCl solution (5%) to achieve pH=7. The epidermoid carcinoma cell line A431 derived from an 85-years-old female with epidermal carcinoma was used for cell culture in order to investigate the biocompatibility characteristics of the nanocomposite.

2.2. Characterization

In order to verify chemical structure of the products, FTIR spectra over a frequency range of 400–4000 cm^{-1} were obtained at room temperature using a FTIR spectrometer (ABB Bomem MB-100). The samples were crushed well and then compressed into examined KBr pellets for all measurements. The thermal properties of the samples were conducted using a thermogravimetric analyzer (TGA-DSC1/Mettler Toledo) ranging from room temperature to 700 ˚C at a rate of 10 ˚C/min under N_2 atmosphere. The surface morphology and thickness of the as-prepared f-rGO sheets were examined by an atomic force microscope (AFM, Veeco) in noncontact mode using a mica base under ambient condition with a scanning rate of 1 Hz. The surface morphology of the composites were observed by scanning electron microscope (SEM) of model Vegall-Tescan and FE-SEM of model Mira 3-XMU. The f-rGO-PVA Hydrogels were allowed to dry; then, the surface of the samples was coated with gold by using a sputter coater (Pishtaz Engineering Co. High Vacuum Technology Center (ACECR- Sharif University Branch-Iran)) before SEM analyses. High resolution transmission electron microscopy (HRTEM) images were carried out by a Philips CM30 electron microscope. The mechanical compression tests of the hydrogels were measured using a universal testing machine (Hounsfield H10ks) at room temperature. The samples were cut into cylindrical shapes (diameter 20 mm and height 10 mm) and the average value of three measurements has been reported. The compression tests were performed under a controlled velocity of clamping of 2 mm/min until failure. For determining of the tensile strength of the film composites, the samples were cut into rectangular shape with width of 10 mm and thickness of 3 mm. The tensile strength measurements were conducted with a Hiwa 200 universal testing machine with a 10 KN load cell and at jaw separation speed of 5 mm/min at room temperature (25˚C). The average amount of

three separate measurements has been reported. XRD analyses of the products were carried out using Rigalcu D/Max-3c X-ray diffractometer with Cu-Kα radiation. The XPS spectra were recorded using a high resolution X-ray spectrometer (Gammadata-Scienta ESCA 200).

In order to determine the amount of water in f-rGO-PVA hydrogels with different loadings of the nanofiller, the samples were dried in a vacuum at 40 ˚C until a constant weight. The water content was calculated using equation (1):

Water content (%) = $(W_0 - W)/W_0 \times 100$ Equation (1)

Where W_0 and W are the weight of f-rGO/PVA hydrogel before and after drying respectively.

In order to determine the swelling ratio, the f-rGO/PVA samples were put into a vacuum at 40 ˚C and dried to a constant weight. The dried samples were immersed in distilled water for 24 hours and then, were removed and their surfaces blotted with filter paper before being weighed. The swelling ratio of f-rGO/PVA nanocomposites was calculated according to the equation (2):

Swelling ratio (%) = $(W - W_0)/W_0 \times 100\%$ (Equation 2)

where W_0 and W are the weight of the hydrogel before and after soaking in water respectively.

2.3. Synthesis of graphene oxide

The modified Hummer's method was used for the synthesis of GO. Briefly, 3 g of purified graphite was loaded in a flask containing 360 mL H_2SO_4 (98%) and 40 mL H_3PO_3. 18 g of $KMnO_4$ was added to the above solution during 30 min and stirred at 50˚C. After 12 hours, distilled water (150 mL) was added and the temperature of the solution fixed in 4 ˚C. Then, 4 mL of H_2O_2 (30%) was added dropwise until the colour change of the solution and as long as there is no bubbles. The achieved solid was washed thoroughly with HCl 5% and water several times.

2.4. Synthesis of salep functionalized reduced GO (f-rGO)

3 g of salep was loaded in mixture solution of butanol (30 mL) and HCl 37% (1.9 mL) then, stirred at 120 ˚C for 20 hours. The resulting solid (hydrolyzed salep) was washed with butanol and dried at 40 ˚C. 0.1 g of hydrolyzed salep was loaded in 25 mL solution of dry DMF and 30 µL of acetic acid (98%). Then, 100 mg of dispersed GO in 10 mL dry DMF was added to the above solution and refluxed at 120 ˚C for 60 hours. The resulting f-rGO was washed with acetone and deionized water several times. **2.5. Preparation of PVA film and hydrogel nanocomposites**

The film nanocomposites were prepared via solution casting method. In a typical procedure, 1.5 g of PVA was dissolved in 15 mL DI water at 90 ˚C. Afterwards, determined amounts of dispersed f-rGO in 10 mL DI water, citric acid and glycerol were added to the solution according to the Table 1. The matrix was stirred for 3 hours and then cast to a petri plate (diameter 9 cm).

For preparation of the hydrogels, an aqueous solution of the PVA (10 %), MBA and f-rGO (according to the Table 2) was stirred at 90 ˚C for 30 min; then, 0.3 g of APS was added and the reaction was kept until the completion of the gelation process.

2.6. Cytotoxicity assay

To evaluate cytotoxicity of the film and hydrogel nanocomposites, MTT colorimetric assay based on general methods was used. For extraction of the products, sterilized

samples (8 cm^3) using UV irradiation were placed in individual wells and added cell culture media in each well and incubated at 37 ˚C for a week.

These media were removed for MTT assay. A431 (human skin cell carcinoma) were seeded at a density of 1×10^4 cells/ml on a 96-well tissue culture polystyrene plate and incubated at 37 ˚C for 24 hours. The extract of the products (at various concentration) were added to the wells and cells cultured for more 24 hours. Then, the culture medium was removed and 100 µL of MTT solution diluted in PBS (0.5 mg/mL) added to the wells. Plate incubated at 37 ˚C for 4 hours. After removal of the medium, isopropanol solution was added to each well in order to complete dissolving of the produced blue crystals. The absorbance was measured at 545 nm using spectrometric microplate reader. The cell viability was calculated by normalization of optical density of the samples to the control. The wells with more alive cells show higher optical density (OD) therefore, the cell viability could be calculated using equation (3) and (4).

Toxicity % = (1 – (mean OD of sample/mean OD of control) × 100 Equation (3)

Table 1 Formulations of the film nanocomposites

Sample code	PVA (g)	Glycerol (g)	Citric acid (g)	f-rGO (wt%)
P	1.5	--	--	--
P*	1.5	--	--	--
P-$G_{3\%}$	1.5	--	--	3
P-$G_{6\%}$	1.5	--	--	6
P-$G_{3\%}$-gly_1	1.5	0.3	--	3
P-$G_{6\%}$-gly_1	1.5	0.3	--	6
P-$G_{3\%}$-ca_1	1.5	--	o.3	3
P-$G_{6\%}$-ca_1	1.5	--	o.3	6
P-$G_{3\%}$-gly_1-ca_2	1.5	o.3	o.5	3
P-$G_{6\%}$-gly_1-ca_2	1.5	o.3	0.5	6
P-$G_{3\%}$-gly_2-ca_1	1.5	o.5	o.3	3
P-$G_{6\%}$-gly_2-ca_1	1.5	o.5	0.3	6
P-gly_1	1.5	o.3	--	--
P-ca_1	1.5	--	o.3	--

*6 wt% of salep was added

Table 2 Formulation, swelling and water content of the hydrogel nanocomposites

					Swelling (%)		Water content (%)	
Sample code	PVA(g)	MBA(g)	APS(g)	f-rGO (g)	pH=7	pH=12	pH=7	pH=12
1	1	0.1	0.3	0	166	193	91.87	93.42
2	1	0.1	0.3	0.02	158	181	92.50	94.35
3	1	0.1	0.3	0.05	197	176	93.82	94.09
4	1	0.1	0.3	0.1	169	180	93.07	94.63
5	1	0.3	0.3	0	140	151	91.47	92.52
6	1	0.3	0.3	0.02	126	167	91.46	93.12
7	1	0.3	0.3	0.05	118	180	91.72	94.05
8	1	0.3	0.3	0.1	120	172	91.94	94.10

Viability % = 100 – T Equation (4)

3. Results

3.1. Preparation of the nanocomposites

Scheme 1, represents the preparation procedure of the film and hydrogel nanocomposites. GO was prepared according to the Hummer's method. Hydrolyzed salep was used simultaneously for the reduction of GO and stabilizing agent for preventing the agglomeration of the rGO sheets. Salep molecular weight decreasing is observed after hydrolysis in gel permeation chromatographs (Fig. 1). According to the previous studies, polyhydroxy materials like cellulose act as a reducing agent for the transformation of GO to rGO [20]. Herein, the hydroxyl groups of salep acted as the mild reducing agent, deoxygenated the exfoliated graphene oxide and also provided strong interactive sites for binding to the rGO nanosheets. The film preparation was performed via simple solution casting method. Salep modification provided homogenous dispersion of the f-rGO and effective mixing between the nanofiller and PVA. Additives like glycerol and citric acid were used in order to obtain desired mechanical performance. Moreover, hydrogels were prepared for the first time via chemical crosslink addition in the absence of the typical toxic acrylate monomers. APS creates hydroxyl radicals on salep and PVA which are crosslinked chemically by MBA. The resulting hydrogels possess high mechanical strength and elasticity as shown in Scheme 1. The reaction was conducted at two different pH (7 and 12) and the swelling data shown in Table 2, confirmed the considerable effect of pH on water absorbency of the dried hydrogel.

3.2. Investigation of the GO reduction

Several methods were used to investigate the reduction of GO through functionalized process with salep. X-ray diffraction of GO and f-rGO are shown in Fig. 2. The XRD pattern of GO shows a sharp peak at 2θ=11° corresponding to the interlayer spacing of 8.03 Å. The peak broadening of 2θ=21.5° (d-spacing 4.13 Å) and 2θ=54° corresponding to the (004) plane of graphene in the f-rGO XRD pattern, indicate the successful reduction of GO. The

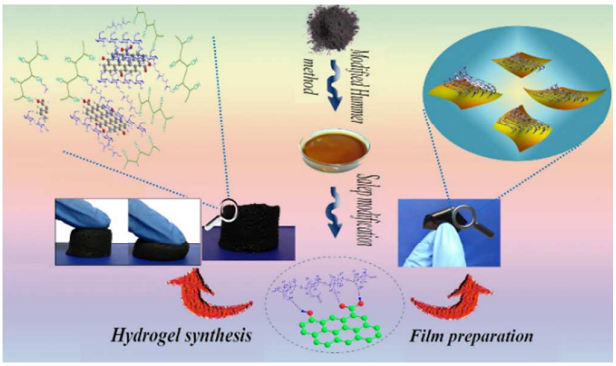

Scheme 1 General procedure for the nanocomposite fabrication

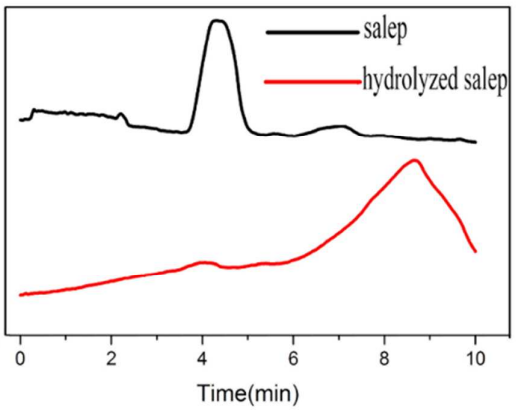

Fig. 1 Gel permission chromatographs of salep and hydrolyzed salep

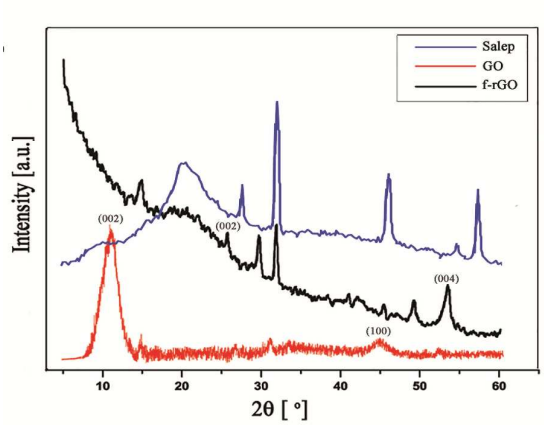

Fig. 2 XRD data for salep, GO and f-rGO of PVA based

XRD peaks of hydrolysed salep are shifted in f-rGO due to interaction with graphene. The reduction of GO with salep was also characterized using UV-Vis spectroscopy. As shown in Fig. 3, GO peak around 240 nm red-shifted to 270 nm in f-rGO. Moreover, the shoulder at 300 nm (n-π* transition of –COOH groups in GO) evidently disappeared due to the formation of conjugated structure of rGO. UV-Vis spectrum of salep demonstrates no significant peak.

Meanwhile, the chemical structure and presence of salep on the surface of f-rGO were evaluated using XPS analysis. The XPS spectrum in the C1s region of f-rGO is depicted in Fig. 4. This spectrum shows five different types of carbon components containing: the sp^2 carbon (284.8 eV) of reduced graphene, sp^3 carbon (285.7 eV), the carbon of C-O (286.8 eV), C=O (287.8 eV) and O-C=O (291.6 eV) which are associated with the residue oxygen function and salep on the surface of f-rGO.

In conclusion, XRD and UV-Vis spectroscopy confirm the reduction of graphene oxide to graphene. Besides, chemical linkage between salep and graphene is interestingly displayed in XPS spectrum.

3.3. FTIR analysis

FTIR analysis is one of the most powerful tools to study the chemical transformations and interactions effectively. FTIR spectra of salep, hydrolyzed salep, GO and f-rGO are shown in Fig. 5. FTIR spectrum of GO contains a broad band at 3233 cm^{-1}, which is related to the hydroxyl groups. The vibrational peaks of carboxylic acid and carbonyl groups are locateded at 1727 and 1622 cm^{-1} respectively. Other bands are also observed at 1397 cm^{-1} (C-OH), 1228 cm^{-1} (C–O–C) and 1058 cm^{-1} (C–O). These characteristic peaks indicate that GO have been successfully

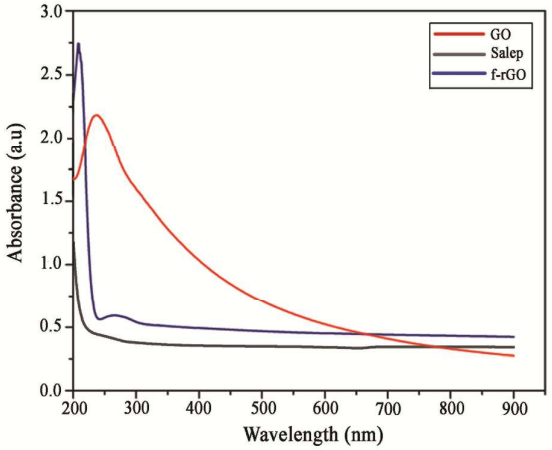

Fig. 3 UV-Vis spectra of GO and f-rGO

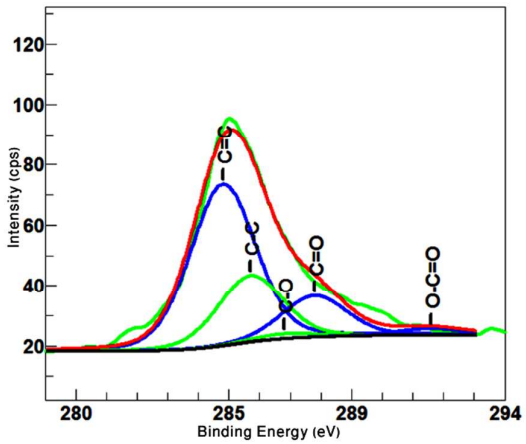

Fig. 4 XPS spectrum of f-rGO

synthesized. The stretching and bending vibrations of salep hydroxyl groups occurs at 3523 and 1687 cm^{-1}, respectively. The bands at 1170 and 1114 cm^{-1} are attributed to the stretching of C–O in C–O–H. The peak at 2947 cm^{-1} is a characteristic band of the C–H stretching. Appearance of the C=O stretching band at 1740 cm^{-1} in FT-IR spectrum of hydrolyzed salep, corresponds to the acyclic structure of the terminal monosaccharides at each oligosaccharide chains which its equilibrium concentration increases after hydrolysis.

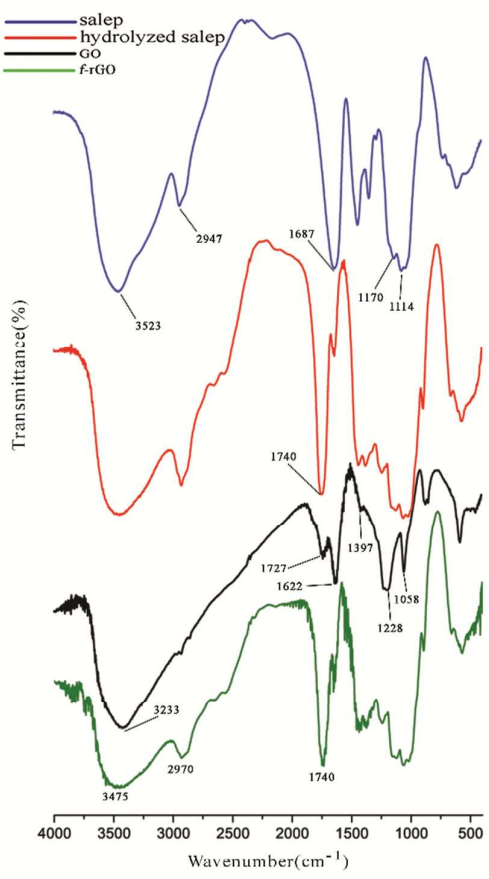

Fig. 5 FTIR spectra of salep, hydrolyzed salep, GO and f-rGO

FT-IR spectrum of f-rGO shows dominant peaks at 3475, 2970 and 1740 cm^{-1} which are similar to those of salep, and confirm the existence of hydrolyzed salep in the surface of the rGO sheets.

3.4. TGA studies

Thermogravimetric analysis is a standard technique to determine the thermal stability and composition of the materials. Herein, it was performed in order to determine whether the addition of f-rGO changes the thermal decomposition behaviour of the nanocomposites or not. The decomposition temperature is an important parameter used in studies of the decomposition process. It defines the upper limit of reagent stability and onset of the decomposition reaction [21]. The initial decomposition temperature (IDT) of the pure PVA and f-rGO are 250.0 and 200.2 ˚C respectively, while that for the f-rGO-PVA film is 310.3 ˚C (Fig. 6a). Comparison between the IDT data shows that the strong interaction between PVA and f-rGO have increased the thermal stability of the nanocomposite relative to the starting materials. The TGA curve of pure PVA shows a rapid weight loss in the temperature range of 250-450 ˚C which is corresponding to the polymer backbone decomposition. The TGA curve of the film nanocomposite (P-$G_{6\%}$) has similar behaviour to that of pure PVA. However, it shows low weight loss in the same temperature region compared to the pure PVA. Therefore, f-rGO addition in low dosages can effectively improves the thermal stability of PVA. Under a nitrogen atmosphere, the residual weight of the samples is related to the amount of carbon, which is 6.81% and 13.60% for pure PVA and P-$G_{6\%}$ respectively. Therefore, f-rGO addition in low dosages increases the residual weight of the film composite. Salep

loading on the surface of the GO is 40% according to the f-rGO TGA curve in Fig. 6a. The hydrogel composites containing f-rGO show similar thermal stability as observed in Fig. 6b. The TGA thermograph of **Sample 3** containing 0.05 g f-rGO (according to the Table 2) shows higher thermal stability than **Sample 1** in the temperature range of 400-700˚C due to the formation of more interfacial interactions between PVA and f-rGO through hydrogen bonding.

3.5. Surface morphology studies

AFM images of the GO and f-rGO on a mica substrate are shown in Fig. 7a and 7b respectively. The thickness of the synthesized GO sheets is 1.4 nm which is higher than that of the theoretical calculated value (0.34 nm)[22]. The average height of the f-rGO

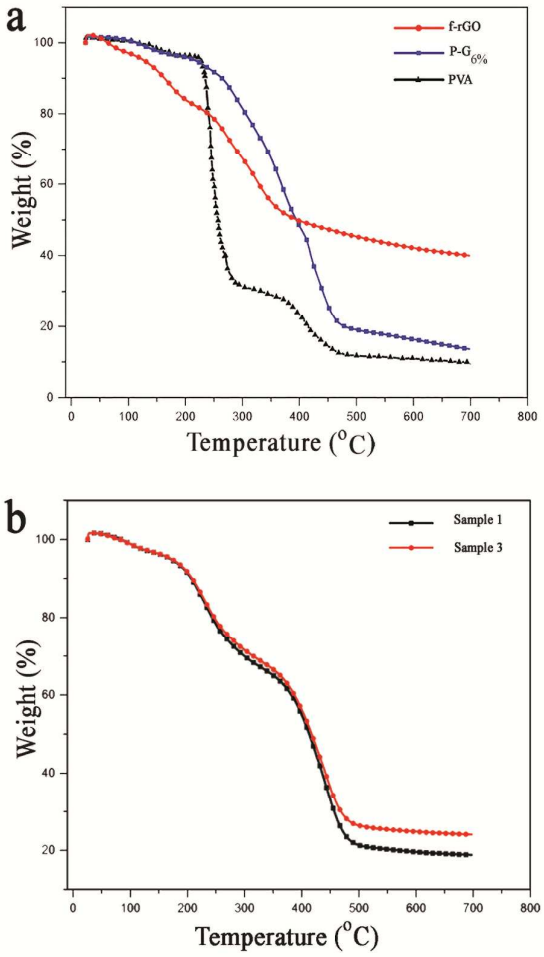

Fig. 6 Thermal properties of the (a) film and (b) hydrogel nanocomposites

sheets is approximately 3 nm which indicates the presence of salep on the surface of the rGO. Fig. 8a and 8b show SEM images of GO and f-rGO respectively. The wrinkle like surface morphology of GO has been transformed to the smooth and planar shape that provided evidences for the effective interaction of salep with GO. The hydrogen bonding between hydroxyl groups of salep/GO and the reproducing of the conjugated structure of f-rGO create surface morphological changes of GO. Fig. 8c shows a SEM cross-section image of the hydrogel (**Sample 4** with composition according to the Table 2). The homogenous dispersion of f-rGO and lamellar structure

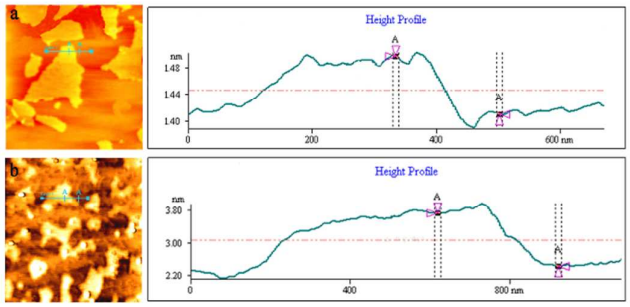

Fig. 7 AFM images and height profiles of single sheet of (a) GO and (b) f-rGO

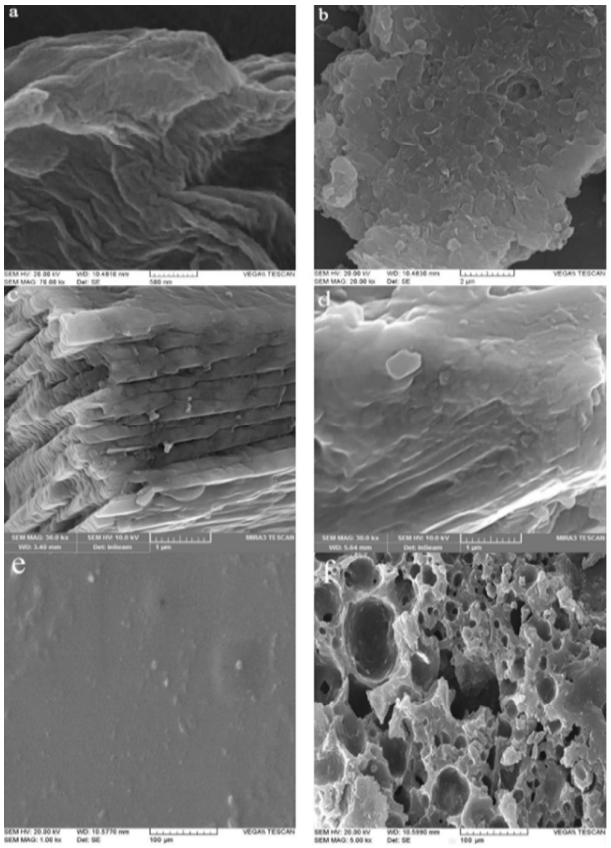

Fig. 8 SEM images of (a) GO (b) f-rGO (c) cross-section and (d) surface of the hydrogel **Sample 4** (e) P-G6% film nanocomposite before and (f) after incubation in water

of the hydrogel exhibit stable dispersion of the nanofiller into the PVA solution. SEM image of the surface of the hydrogel **(Sample 4)** is observed in Fig. 8d. It is clear that f-rGO was sandwiched between PVA layers; mainly because of the regular hydrogen bonding formation between PVA and f-rGO. SEM images of the film nanocomposites (P-$G_{6\%}$) before and after incubation in water are shown in Fig. 8e and Fig. 8f respectively. The swelled film was freeze-dried and the porous structure indicates that the nanocomposites have the ability to transform the water soluble materials which is crucial in tissue engineering scaffolds.

Fig. 9 shows the TEM images of the film nanocomposite reinforced with f-rGO displaying that f-rGO is indeed present in the polymer matrix and is covered by polymer molecules.

3.6. Mechanical studies of the nanocomposites

The mechanical characteristics of hydrogels such as compressive strength have important role for their medicinal applications especially tissue engineering.[23] The typical force-compression diagrams of the synthesized hydrogel nanocomposites have been plotted in Fig. 10. These analyses provide evidences that whether the f-rGO/PVA hydrogels have appropriate mechanical features for tissue scaffold mimicking or not. The effects of different contents of f-rGO and cross-linker on the mechanical parameters of the hydrogels were examined and the calculated data listed in Table 3. The compressive modulus were calculated at 65% of the compression. It is apparent that addition of 0.1 g f-rGO (**Sample 4**) has improved the compressive strength and Young's modulus 25.7% and 77% respectively compared to the **Sample 1**. These results confirm the homogenous dispersion of f-rGO on the

Table3 Calculated mechanical parameters of the hydrogel nanocomposites

Sample code	Strength (kPa)	Compression (%)	Modulus (kPa)
1	223	82	229.3
3	141	89.5	45.8
4	300	85.1	1000
5	173	69.6	71.3
Ref [24]	300-450	-	102-136
Ref [25]	500-3500	-	15-67
Ref [26]	7-24	-	125-828

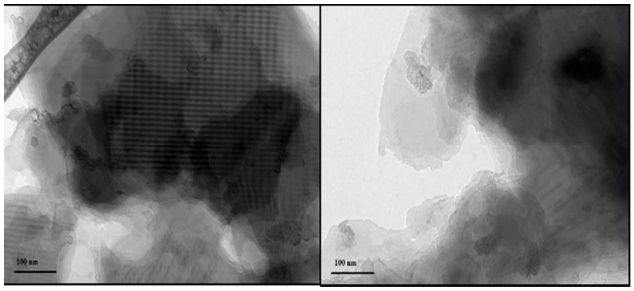

Fig. 9 TEM images of PVA/f-rGO nanocomposite

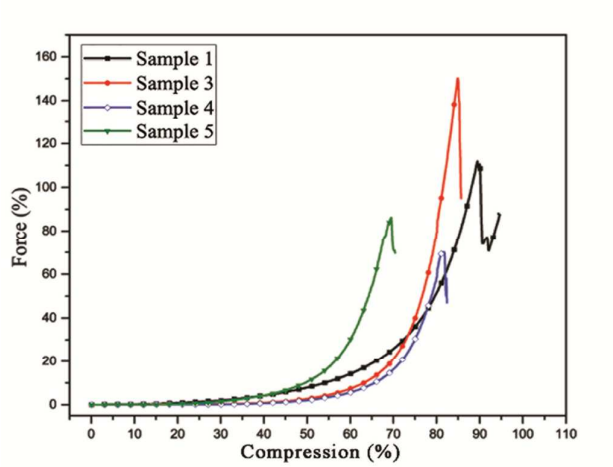

Fig. 10 Compressive mechanical tests of the synthesized hydrogels

hydrogel matrix. Moreover, the higher value of MBA, the more brittle hydrogel formation (**Sample 5**).

In summary, the enhancement of mechanical characteristics of the hydrogels is obtained through reinforcement effect of f-rGO on PVA and using lower amount of MBA in the hydrogels. We have compared the mechanical properties of our hydrogel with those of other PVA based hydrogels which have been also used in tissue engineering (Table 3). In these studies, other components such as clay[24], monomers with acrylate functions[25] and two cross-linker agents[26] have been used for the improvement of the mechanical strength. It is clear that the mechanical properties included in our study can be tailored for the variety of soft tissue applications.

The film nanocomposites were prepared with different amounts of the additives in order to achieve appropriate mechanical characteristics for soft tissue scaffolds. Therefore, effects of the f-rGO, glycerol and citric acid addition on the mechanical properties were studied. The typical tensile stress/elongation graphs of the film nanocomposites and the calculated mechanical parameters are shown in Fig. 11 and Table 4 respectively.

There are some comparison data between this work and reported data at the end of the Table 4. The synthesized nanocomposite are flexible with tensile strength ranging from 14.39 to 70.51 MPa and breaking elongation from 26.17 to 650.51%.

Salep has decreased the tensile strength of the film from 54.48 to 37.1 MPa due to make changes in the crystallinity of PVA. However, importing of salep in the form of f-rGO has increased the tensile strength from 54.48 to 70.51 MPa. f-rGO lies between polymer chains because of interlayer adhesion and makes more uniform stress distribution that this improves the strain strength of the composite. In the other hand,

addition of more f-rGO has decreased the tensile strength to 62.43 MPa

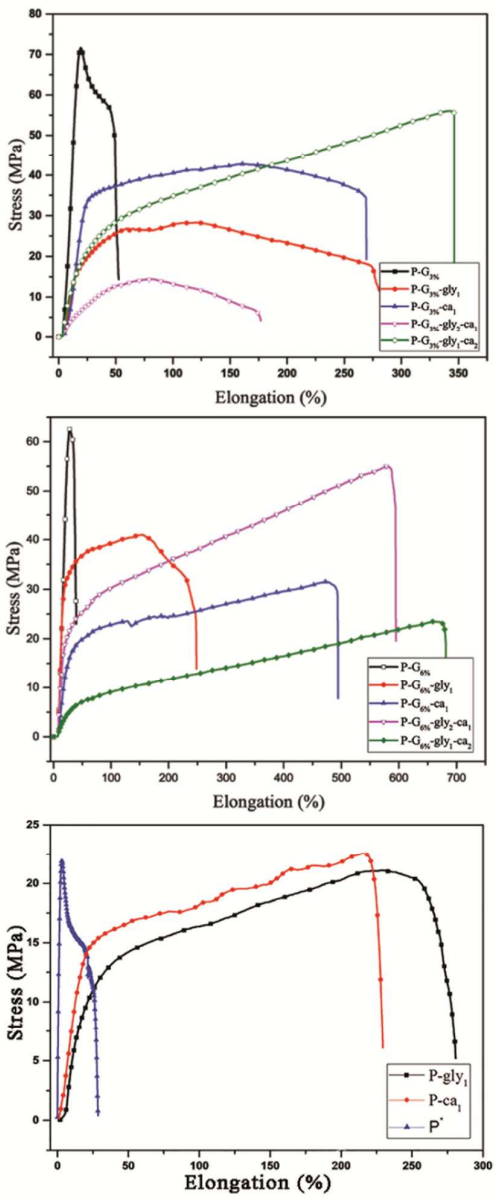

Fig. 11 Tensile behaviour of the films with different loading of f-rGO and other additives

due to stacking of graphene layers. On the other hand, f-rGO increases the loading of salep in the nanocomposites which improves cell adhesion consequently. Therefore, we aimed by using materials such as glycerol and citric acid to overcome the mechanical drawbacks of high dosages of f-rGO. Glycerol increased the elongation at break and produced flexible films due to its plasticizing effect but decreased the tensile strength strongly. Consequently, the mechanical properties were studied with respect to the citric acid addition which have been used frequently at biomaterials because of its biocompatibility. [34] Citric acid decreased polymer chain mobility through creating cross-linked bonds and improved of the tensile strength via better intermolecular interactions between the components. Finally, effects of the both additives on the mechanical properties of the film composites were examined. As seen in Table 4, the film nanocomposite with 6 wt%, 0.3 g and 0.5 g of f-rGO, citric acid and glycerol respectively, is elastic and amenable to the mechanical requirements that might be desirable during tissue development.

Comparing the reported data of the other film nanocomposites with same applications as well as soft tissues at the end of Table 4, we have succeed to enhance the tensile strength and elasticity of the samples considerably.

Table 4 Mechanical parameters of the film nanocomposites

Sample	Tensile strength (MPa)	Elongation at break (%)	Modulus (MPa)
P	54.48	122	3.78
P*	37.1	22.31	32
P-$G_{3\%}$	70.51	57.23	0.345
P-$G_{6\%}$	62.43	26.17	0.32
P-$G_{3\%}$-gly_1	28.2	213.45	1.94
P-$G_{6\%}$-gly_1	40.86	176.38	3.38
P-$G_{3\%}$-ca_1	42.57	211.22	1.50
P-$G_{6\%}$-ca_1	31.47	197.13	1
P-$G_{3\%}$-gly_1-ca_2	55.65	332.76	2.31
P-$G_{6\%}$-gly_1-ca_2	23.23	650.51	0.34
P-$G_{3\%}$-gly_2-ca_1	14.39	195.1	0.71
P-$G_{6\%}$-gly_2-ca_1	54.52	432.19	2.72
P-gly_1	21.04	248.55	1.07
P-ca_2	40.34	212.96	0.56
Ref [27]	9.2-29	660-895	-
Ref [28]	22.67	95.8	323.15
Ref [29]	14.2-27	554-802	209-442
Ref [30]	-	-	0.3-0.8
Ref [31]	33.53	239	115
Ref [32]	0.142	22.5	1.47
Ref [31]	16.77	418	11
Ref [33]	20	269	-
Ref [23]	0.403	33.4	3.5
Tendon[25]	50-100	10-15	-
Ligament aorta[25]	0.3-0.8	50-100	-
Skin[25]	1-20	30-70	-
Skin[28]	5-30	35-115	15-150
Articular cartilage[25]	9-40	60-120	-

3.7. Swelling studies

Swelling ratio and water content are important properties that must be considered in the composites used in tissue scaffolds. The hydrophilicity character of the bulk composite can determine the overall permeation of nutrients into and cellular products out of the scaffold and its biodegradation rate as well. Moreover, large inner surface area of the artificial scaffolds which is crucial for the attachment, proliferation and migration of cells could be related to the water absorption percent. The swelling ratio of the film nanocomposites are shown in Fig. 12.

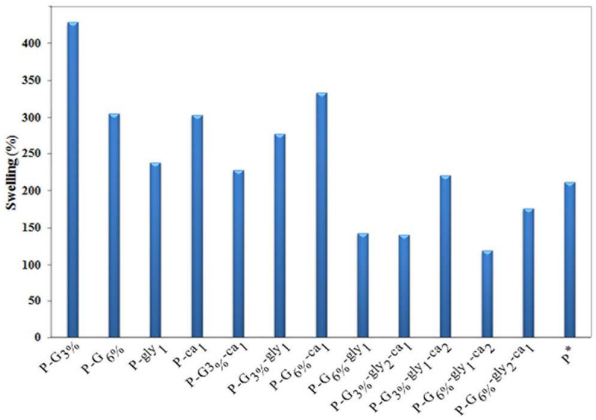

Fig. 12 Swelling ratio of the film nanocomposites

In general, citric acid addition and using lower amount of f-rGO have improved the swelling ratio, but glycerol had no significant effect. Citric acid improved the swelling ratio of the film containing 6 wt% of f-rGO to 134% because of the carboxylic acid groups which have increased the hydrophilic character of the film composite. In contrast, in the sample

containing 3 wt% of f-rGO, citric acid addition decreased the swelling ratio, probably because of citric acid cross-linking and lowering the free volume of water uptake sites. In comparison with other reported data, these nanocomposites have considerable swelling ratio which is suitable for their applications as soft tissue scaffolds.

The calculated swelling ratio and water content of the synthesized hydrogels are listed in Table 2. For accurate investigation of the swelling ratio, this parameter have been calculated according to the full factor consideration (the amount of MBA, f-rGO and initial pH of the solution) and the signal to noise (S/N) ratio of each factor are given in Table 5: the higher value of the S/N ratio, the more water uptake of the hydrogel.

Table 5 Synthetic conditions effect on swelling ratio of the hydrogels

	pH		MBA (g)		f-rGO (g)			
	7	12	0.1	0.3	0	0.02	0.05	0.1
S/N ratio	5.70	15.20	14.38	6.41	7.08	6.94	4.88	5.89

The swelling ratio of the hydrogels with higher MBA values have decreased because of small pore sizes compared to the hydrogels with lower amount of cross-linker. Synthesis of the hydrogels in basic solution, have increased the water uptake due to the generating of anionic R–O- groups in the backbone of the hydrogel. The effect of f-rGO amount on the swelling ratio is almost complicated. The polar hydroxyl groups of salep and non-polar graphene structure have the opposite effect on the water absorption. When f-rGO is increased from 0.02 to 0.05 the S/N ratio is decreased due to the hydrophobic structure of graphene. However, at f-rGO=0.1 the S/N ratio is increased because the hydrophilic structure of salep overcome to the graphene non-polar effect. It is notable that both desired mechanical performance and optimum swelling ratio have been achieved when f-rGO=0.1.

3.8. Cytotoxicity studies

Cell viability was measured using MTT assay that is represented in Fig. 13. The cell viability numbers over 80 % for the P-$G_{6\%}$-gly_2-ca_1 sample at two different concentration represented non-toxic and highly biocompatible properties of the films. The cell viability results based on the in vitro MTT method for the hydrogel samples **1** and **4** are shown in three different concentrations (**Sample 1''** is 10 times diluted than **Sample 1'** which is 10 times diluted than **Sample 1**). Therefore, the synthesized f-rGO has no harmful effect on the PVA based nanocomposites, which is a primary concern for their applications in artificial tissue constructs *in vivo*.

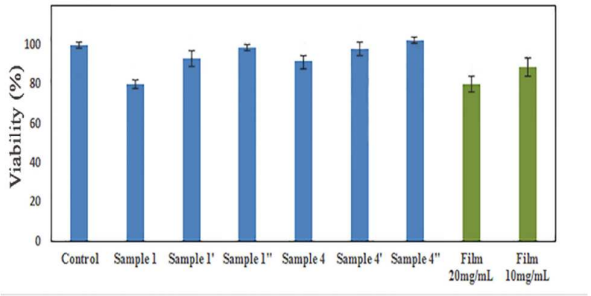

Fig. 13 Cell viability of the nanocomposites at different concentration

3.9. Discussion

Herein, PVA based nanocomposites have been fabricated and investigated as the biomaterials for construction of artificial scaffolds. The major concern in this area is the fabrication of the scaffolds with high elasticity and strength coupled with controllable biodegradation, cell-viability and pore morphology, all depending on the type of tissue. For example, porosity and high strength are most important features in skin and bone regeneration respectively or pliability are required for blood vessels and intestine in order to achieve flexible matrix forms. Poly (vinyl alcohol) is extensively used in biomedical applications due to its slow degradability, good biocompatibility and desired mechanical characteristics. While, the cell affinity of the synthesized polymers are poor, polysaccharides are integral component of many cells and proteins because of their carbohydrate moiety. In this study, we used salep and other additives in order to improve the characteristics such as swelling ratio, elasticity or porosity of the films and hydrogels. According to the Table 4, addition of the f-rGO enhanced the ultimate tensile strength and elongation at break in the P* films. Furthermore, the value of modulus has been decreased by using glycerol and citric acid additives indicating high elasticity which is an important factor for soft tissue scaffolds handling.

The synthesized hydrogels in this work have many advantages compared to the previously reported PVA based hydrogels. Herein, we avoid doing time consuming freeze/thaw methods which need very low temperature (-22 ^{o}C)[35] or toxic acrylate monomers[36] which is usually used for hydrogel synthesis. The reported data listed in Table 2, show that the presence of salep in f-rGO has improved water content and swelling ratio of the hydrogels along with good mechanical properties associated by graphene. The suitable modulus for the soft scaffolds is 600-1600 KPa[37] that for our hydrogels ranging from 0.1-1 MPa at full hydrated state to 0.5-3.5 MPa for the dry films.

The water uptake of the films and hydrogels ranged from 114-428 and 91-197 respectively. These values are comparable with soft tissues which contain 60-80% of water. Besides, the cell viability test via MTT reducing assay have demonstrated that these materials are able to be employed for cell growth and proliferation successfully.

4. Conclusion

In this study, we aimed to fabricate scaffolds for tissue engineering applications based on PVA. Salep functionalized reduced graphene oxide was used as a reinforcing agent for the nanocomposite structures. The 3D-nanocomposite in both of the film and the hydrogel constructs were made and characterized thoroughly. These biocompatible nanocomposites displayed mechanical strength, flexibility and suitable swelling ratio which could be tailor by using f-rGO and other additives.

References

1 M. Kita, Y. Ogura, Y. Honda, S. Hyon, W. Cha and Y. Ikada, *Graefe's Arch Clin Exp Ophthalmol*, 1990, **228**, 533-537.

2 B. Singh and V. Sharma, *Int. J. Pharm.,* 2011, **389**, 94–106.

3 M. I. Baker, S. P. Walsh, Z. Schwartz and B. D. Boyan, *J. Biomed. Mater. Res., Part B*, 2012, **100**, 1451-1457.

4 M. Kobayashi, J. Toguchida and M. Oka, *Biomaterials, 2003,* **24**, 639–647.

5 Y. Zhu, S. Murali, W. Cai, X. Li, J. Suk, J. R. Potts and R. S. Ruoff, *Adv. Mater*., 2010, **22**, 3906-3924.

6 Z. Sui, X. Zhang, Y. Lei and Y. Luo, *Carbon,* 2011, **49**, 4314-4321.

7 S. Pei and H.Cheng, *Carbon*, 2012, **50**, 3210-3228.

8 H. Shen, L. Zhang, M. Liu and Z. Zhang, *Theranostics,* 2012, **2**, 283-294.

9 C. He, Z. Shi, L. Ma, C. Cheng, C. Nie, M. Zhoua and C. Zhao, *J. Mater. Chem. B*, 2015, **3**, 592–602.

10 J. Texter, *Curr. Opin. Colloid Interface Sci.,* 2014, **19**, 163–174.

11 J. Zhao, Z. Wang, J. C. White and B. Xing, *Environ. Sci. Technol.*, 2014, **48**, 9995–10009.

12 S. Wang, H. Li, L. Zhang, B. Li, X. Cao, G. Zhang, S. Zhang and L. Wu, *Chem. Commun.,* 2014, **50**, 9700-9703.

13 N. B. Shelkea, R. Jamesa, C. T. Laurencina and S. G. Kumbara, *Polym. Adv. Technol.* 2014, **25**, 448–460.

14 A. Chhatri, J. Bajpai and A.K. Bajpai, *Biomatter,* 2011*,* **1**, 189-197.

15 A. Pourjavadi, G. R. Bardajee and R. Soleyman, *J. Appl. Polym. Sci.,* 2009, **112**, 2625-2633.

16 M. Tiana, L. Qua, X. Zhang, K. Zhang, S. Zhua, X. Guoa, G. Hana, X. Tanga and Y. Sun, *Carbohydr. Polym.*, 2014, **111**, 456–462.

17 X. Feng, X. Wang, W. Xing, B. Yu, L. Song and Y. Hu, *Ind. Eng. Chem. Res.*, 2013, **52**, 12906–12914.

18 N. Georgiadis, C. Ritzoulis, E. Charchari, C. Koukiotis, C. Tsioptsias and C. Vasiliadou, *Food Hydrocolloids,* 2012, **28**, 68-74.

19 G. R. Bardajaee, A. Pourjavadi, S. Ghavami, R. Soleyman and F. Jafarpour, *J. Photochem. Photobiol. B.,* 2011, **102**, 232-240.

20 H. Peng, L. Meng, L. Niu, Q. Lu, *J. Phys. Chem. C,* 2012, **116**, 16294−16299.

21 B. V. L'vow, Thermal Decomposition of Solids and Melts: New Thermochemical Approach to the Mechanism, Kinetics and Methodology, Springer, Hungary, 2007, ch. 5, pp. 65.

22 X. Ling, J. Wu, L. Xie and J. Zhang, *J. Phys. Chem. C,* 2013, **117**, 2369−2376.

23 Y. Xiao, E. A. Friis, S. H. Gehrke and M. S. Detamore, *Tissue Eng Part B Rev*., 2013**, 19**, 403–412.

24 S. Sharifi, S. B.G. Blanquer, T. G. van Kooten and D. W. Grijpma, *Acta Biomater.,* 2012, **8**, 4233–4243.

25 D. T. Padavan, A. M. Hamilton, L. E. Millon, D. R. Boughner and W. Wan, *Acta Biomater.*, 2011, **7**, 258–267.

26 R. H. Schmedlen, K. S. Masters and J. L. West, *Biomaterials*, 2002, **23**, 4325–4332.

27 J. Guan, M.S. Sacks, E. J. Beckman and W. R. Wagner, *J. Biomed. Mater. Res., Part A,* 2002, **61**, 493-503.

28 W. Li, C. T. Laurencin, E. J. Caterson, R. S. Tuan and F. K. Ko, *J. Biomed. Mater. Res., Part A*, 2002, **60**, 613-621.

29 C. Wan and B. Chen, *Biomed. Mater.,* 2011, **6**, 055010.

30 M. I. Baker, S. P. Walsh, Z. Schwartz and B. D. Boyan, *J. Biomed. Mater. Res., Part B,* 2012, **100**, 1451-1457.

31 L. V. Thomas, U. Arun, S. Remya and P. D. Nair*, J. Mater. Sci. Mater. Med.,* 2009, **20**, 259–269.

32 N. Mohan and P. D. Nair, *J. Biomed. Mater. Res., Part B*, 2008, **84**, 584-594.

33 E. S. Costa-Júnior, E. F. Barbosa-Stancioli, A. A.P. Mansur, W. L. Vasconcelos and H. S. Mansur, *Carbohydr. Polym.,*2009, **76**, 472–481.

34 N. Reddy and Y. Yang, *Food Chem.*, 2010, **118**, 702–711.

35 L. Zhang, Z. Wang, C. Xu, Y. Li, J. Gao, W. Wang and Y. Liu, *J. Mater. Chem*., 2011, **21**, 10399–10406.

36 D. T. Padavan, A. M. Hamilton, L. E. Millon, D. R. Boughner and W. Wan, *Acta Biomater.*, 2011, **7**, 258–267.

37 J. You, M. Rafat, G. J. C. Ye and D. T. Auguste, *Nano Lett.,* 2011, **11**, 3643–3648.